

This document is downloaded from DR-NTU, Nanyang Technological University Library, Singapore.

Title	Optical characteristics of 1.55 m GaInNAs multi-quantum wells(Published version)
Author(s)	Sun, Handong; Clark, Antony H.; Liu, H. Y.; Hopkinson, M.; Calvez, Stephane; Dawson, M. D.; Qiu, Y. N.; Rorison, J. M.
Citation	Sun, H. D., Clark, A. H., Liu, H. Y., Hopkinson, M., Calvez, S., Dawson, M. D., et al. (2004). Optical characteristics of 1.55 mm GaInNAs multi-quantum wells. Applied Physics Letters, 85(18), 4013-4015.
Date	2004
URL	http://hdl.handle.net/10220/6060
Rights	Applied Physics Letters © copyright 2004 American Institute of Physics. The journal's website is located at http://apl.aip.org/ .

Optical characteristics of 1.55 μm GaInNAs multiple quantum wells

H. D. Sun^{a)} and A. H. Clark

Institute of Photonics, University of Strathclyde, Wolfson Centre, 106 Rottenrow, Glasgow, G4 0NW, United Kingdom

H. Y. Liu and M. Hopkinson

Department of Electronic & Electrical Engineering, EPSRC National Centre for III-V Technologies, University of Sheffield, Sheffield, S1 3JD, United Kingdom

S. Calvez and M. D. Dawson

Institute of Photonics, University of Strathclyde, Wolfson Centre, 106 Rottenrow, Glasgow, G4 0NW, United Kingdom

Y. N. Qiu and J. M. Rorison

Centre for Communications Research, University of Bristol, Bristol, BS8 1TR, United Kingdom

(Received 22 June 2004; accepted 1 September 2004)

We report the optical characterization of high-quality 1.55 μm $\text{Ga}_x\text{In}_{1-x}\text{N}_y\text{As}_{1-y}$ multi-quantum wells (MQWs), grown on GaAs with $\text{Ga}(\text{In})\text{N}_{0.01}\text{As}$ spacer layers. The transitions between the quantized QW states of the electrons and holes have been identified using photoluminescence excitation spectroscopy. Their energies are consistent with theoretical fitting based on the band anticrossing model. It is also confirmed by detailed spectroscopic measurements that the addition of even a small amount of In to $\text{GaN}_{0.01}\text{As}$ barriers remarkably improves the optical characteristics of the QWs. The results imply that although strain-compensated GaInNAs MQWs provide a feasible approach to realizing 1.55 μm optical emission, the relative lattice mismatch between the wells and barriers is critical to the optical quality of the related QWs. © 2004 American Institute of Physics. [DOI: 10.1063/1.1812371]

Dilute nitride III–V alloy semiconductors, and in particular GaInNAs quaternary compounds, are being intensively investigated as promising active materials for the 1.3–1.6 μm wavelength region, by virtue of advantages including improved temperature-dependent characteristics and feasibility of monolithic integration with AlAs/GaAs based Bragg reflectors.¹ However, with the introduction of N, formation of nonradiative recombination centers appears inevitable and the photoluminescence (PL) efficiency decreases rapidly with increase of N content. As a low N content is therefore preferred, the operation wavelength of most devices utilizing GaInNAs/GaAs multi-quantum wells (MQWs) is still limited to around 1.3 μm .^{2–6}

Extending the operating wavelength of this material system to 1.55 μm is very desirable. Although there have been some initial reports on the demonstration of pulsed laser diodes emitting around $\sim 1.5 \mu\text{m}$,^{7,8} very little has been reported regarding the optimization of growth conditions to realize 1.55 μm PL.^{9–11} Detailed optical characterization, especially regarding the electronic state structures in this material system, is generally very limited and only focused on 1.3 μm samples.^{12–17} In this letter we report the observation of two-dimensional (2D) QW transitions in high-quality 1.55 μm GaInNAs MQWs with $\text{Ga}(\text{In})\text{N}_{0.01}\text{As}_{0.99}$ spacer layers, by means of PL excitation spectroscopy (PLE). In addition, the influence of barrier compositions on the optical properties of these structures has been clarified by detailed spectroscopic measurements.

The samples used in this study comprised three-period QWs sandwiched between 200 nm GaAs and 100 nm AlGaAs layers, and were grown on semi-insulating GaAs

(001) substrates by MBE. Each QW was of nominal well-width 8 nm and composition $\text{Ga}_{0.62}\text{In}_{0.38}\text{N}_{0.03}\text{As}_{0.97}$, grown between 52 nm $\text{In}_{xb}\text{Ga}_{1-xb}\text{N}_{0.01}\text{As}_{0.99}$ spacer layers (barriers). After growth, the samples were annealed *in situ* at 660 °C for 1 h. The detailed growth conditions and their optimization can be found elsewhere.¹¹ Here we focus on comparative studies of two samples with different barrier compositions. In sample A, the barriers are tensile-strained $\text{GaN}_{0.01}\text{As}_{0.99}$ and therefore compose strain-compensating layers to the compressively strained QWs, while in sample B 2.3% In has been added into the $\text{GaN}_{0.01}\text{As}_{0.99}$ barriers so that they are almost lattice-matched to the GaAs substrate. Both samples demonstrate reasonably strong PL around 1.55 μm at room temperature.¹¹

Figure 1 shows the PL spectra under excitation at 670 nm from the dispersed lamp together with PLE spectra of the two samples. Both PLE spectra reveal absorption profiles typical of QWs, namely the step-like structure and the independence of the transition energies on the detection wavelength (not shown here). The crystal quality of these two samples can be compared from the broadening of the PL line shapes. Full widths at half maxima are 26.9 and 15.7 meV, respectively, for samples A and B, indicating the better quality of sample B.

In order to identify the electronic states, we performed calculations of the band structures based on the band anticrossing model in which the localized N states interact with the extended states in the conduction band, taking strain effects into account.^{17–19} The band alignments of all layers are In-content dependent and the band offset in $\text{Ga}_{1-x}\text{In}_x\text{As}/\text{GaAs}$ system with $x=38\%$ was chosen to be 0.8/0.2.²⁰ The valence band structure was solved using the Luttinger–Kohn Hamiltonian.¹⁷ We start with sample B because it has higher crystal quality. Supposing the QWs to be

^{a)} Author to whom correspondence should be addressed; electronic mail: handong.sun@strath.ac.uk

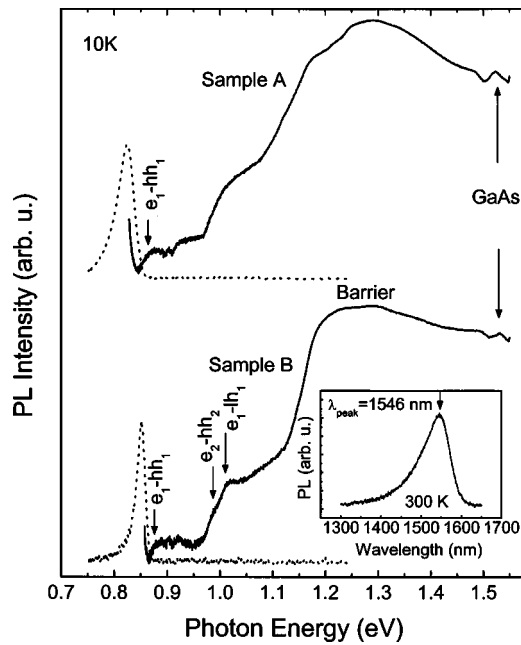


FIG. 1. Typical spectra of PL (dotted lines) and PLE (solid lines) measured at 10 K from two $\text{In}_{0.38}\text{Ga}_{0.62}\text{N}_{0.03}\text{As}_{0.97}$ QW samples with different barrier compositions. The inset shows the PL spectrum of sample B at 300 K.

fully strained (no lattice relaxation), we calculated the QW transition energies using different coupling strength β between the localized N states and the extended states. The calculated transition energies with $\beta=2.45$, which is close to the reported values of other authors,²¹ have been denoted in the PLE curve in Fig. 1. It can be seen that the theoretical fitting is in good agreement with the experimentally observed features. It should be pointed out that the $e_2\text{-hh}_2$ and $e_1\text{-lh}_1$ transition energies are very close so that the $e_2\text{-hh}_2$ transition is not very pronounced and only appears as “a shoulder.” As the GaInNAs/GaAs material system is subject to strong phase separation and in extreme cases the electronic states may demonstrate quantum dot-like features,^{22–24} the demonstration of 2D QW states verifies the high degree of crystallinity in this 1.55 μm material.

A noticeable feature demonstrated in Fig. 1 is that the lowest QW transition energy in sample A is about 26 meV lower than in sample B. This is contrary to expectation, because the barrier confinement in sample A is slightly greater than in sample B (due to the addition of In), therefore the confinement energy and the corresponding transition energy should be higher accordingly. As these two samples are grown under the same conditions and the structures are the same except for the barrier compositions, the anomaly of the transition energy may suggest that the bigger mismatch between the compressed QW/tensile barrier interface in sample A has led to strain relaxation in the QW layers.^{25,26} Actually our calculations show that if we assume 20% lattice relaxation (80% strained) the calculated transition energies coincide with the experimental observation very well.

The improvement of structure quality in sample B is further evidenced by the temperature-dependent PL peak energy behavior shown in Fig. 2. It can be seen clearly that the PL energies in sample A demonstrate the so-called “S-shape” characteristic (redshift/blueshift/redshift) observed extensively in various material systems and considered to be a typical feature of strong localization. For QW samples, the

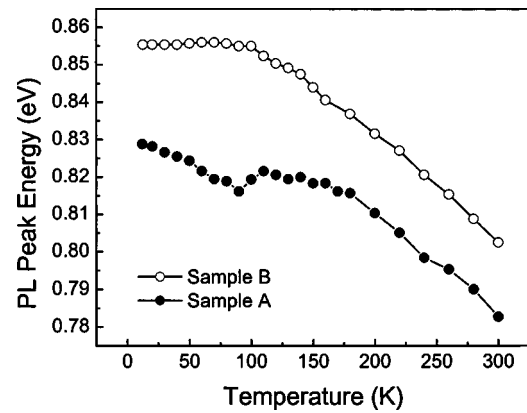


FIG. 2. Temperature dependence of the spectral positions of the PL maxima for two $\text{In}_{0.38}\text{Ga}_{0.62}\text{N}_{0.03}\text{As}_{0.97}$ QWs with different barrier compositions.

localization effect may originate from potential fluctuations due to compositional inhomogeneity and interface roughness. It is noteworthy that this behavior has been largely suppressed in sample B with $\text{Ga}_{0.977}\text{In}_{0.023}\text{N}_{0.01}\text{As}_{0.99}$ barriers.

In order to gain further insight into the effects of the barriers on the optical properties, we performed PL measurements under selective excitation energies for both samples. Figure 3 shows the PL spectra, normalized at their main peaks, under excitation at different energies. It can be seen clearly that for sample B the PL characteristics are barely changed with the excitation energy. For sample A, however, the PL spectra are more sensitively dependent on the excitation energy. When the excitation energy is reduced to be lower than the GaAs band gap, a new emission band appears which is located on the high-energy side of the main QW PL peak (main spectrum and inset). Notably, the peak energy of the new emission band decreases with decrease of the excitation energy and the relative intensity increases when the excitation energy approaches the barrier transition edge. The above-noted features suggest that the new emission band is associated with the barriers and may be attributed to defect-related states generated in the QW/barrier interfaces. In fact,

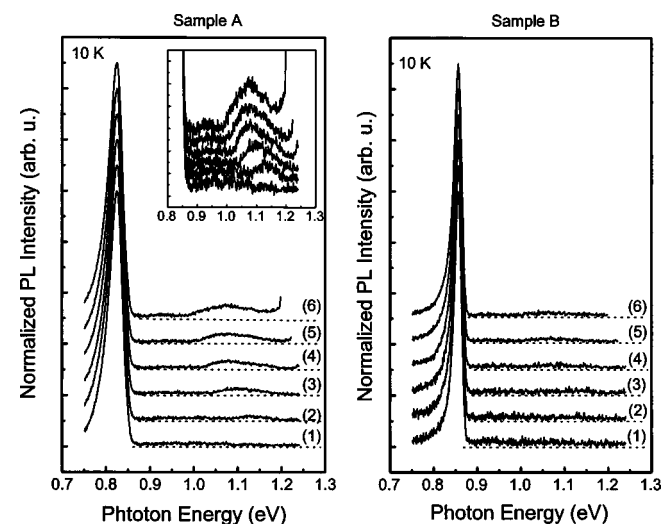


FIG. 3. Normalized PL spectra under different excitation energies. The excitation energies for curves 1–6 are 1.851, 1.378, 1.305, 1.265, 1.240, 1.216 eV, respectively. The dotted straight lines denote the baselines for each spectrum. The inset highlights the emission band near 1.1 eV of sample A.

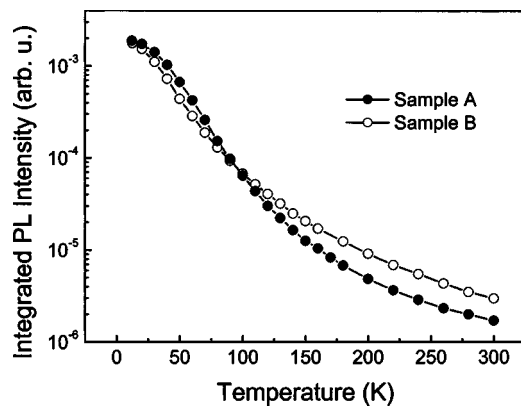


FIG. 4. Temperature dependence of integrated PL intensity for two $\text{In}_{0.38}\text{Ga}_{0.62}\text{N}_{0.03}\text{As}_{0.97}$ QWs with different barrier compositions.

it has been observed that in strain-balanced $\text{In}_x\text{Ga}_{1-x}\text{As}/\text{In}_y\text{Ga}_{1-y}\text{As}$ MQWs if the mismatch between the wells and barriers exceeds a critical limit, morphological or compositional fluctuations may take place in the structure, which can lead to a local structure breakdown with the generation of extended defects.^{27,28} This defect-related emission band vanishes when the excitation energy is too high (see curves 1 and 2) because in this situation the generated carriers are more energetic and harder to be captured by the defect-related states in the barriers. The structural defects make an extra contribution to the broadening of the PL linewidth in sample A, which is in agreement with the PL features. We point out that the evolution of structural defects is a complex phenomenon connected with related energy and kinetics and the correlation of the local structure breakdown with the relative lattice-mismatch between the QWs and barriers should be different for different material systems. The high sensitivity of the structural quality of GaInNAs QWs to the relative mismatch between the QWs and barriers may correlate to intrinsic properties of inhomogeneity due to the fluctuation of local composition, bond configuration, and strain.

Finally, we investigate the effects of the barriers on the relative radiative efficiency. The integrated PL intensities as a function of temperature for samples A and B are shown in Fig. 4. One can see that whilst at low temperature the PL intensity of sample A is comparable to (a little higher than) sample B, the radiative efficiency is opposite at high temperatures. Taking a detailed look at the PL efficiency as a function of temperature, it is noted that the PL quenching rates for these two samples demonstrate different behavior, being slower for sample A than for sample B at low temperature, but opposite at high temperature. It is well known that at low temperatures the PL is dominated by radiation from localized carriers (excitons). In this situation the temperature quenching of PL is ascribed to the thermal activation of carriers from localized states to delocalized QW states where they have more chance to be trapped by defects and recombine nonradiatively. As we have pointed out, sample A has deeper localization energy than sample B, therefore the thermal escape of localized carriers is more difficult than in sample B, which can account for the slower quenching rate in sample A at low temperature. On the other hand, at higher temperature (over 100 K), the PL is dominated by the radiative recombination of free carriers, and the quenching of PL

can be ascribed to the thermal escape of carriers out of the QW ground states. The quenching rate should be dependent on the density of defects.²⁹ Therefore, the faster quenching rate in sample A at high temperature should be related to the higher defect density, which is consistent with the observations in the selectively excited PL spectra.

- ¹M. Kondow, K. Uomi, A. Niwa, T. Kitatani, S. Watahiki, and Y. Yazawa, *Jpn. J. Appl. Phys., Part 2* **35**, 1273 (1996).
- ²T. Kitatani, M. Kondow, S. Nakatsuka, Y. Yazawa, and M. Okai, *IEEE J. Sel. Top. Quantum Electron.* **3**, 206 (1997).
- ³S. R. Kurtz, A. A. Allerman, E. D. Jones, J. M. Gee, J. J. Banas, and B. E. Hammons, *Appl. Phys. Lett.* **74**, 729 (1999).
- ⁴M. C. Larson, M. Kondow, T. Kitatani, K. Nakahara, K. Tamura, H. Inoue, and K. Uomi, *IEEE Photonics Technol. Lett.* **10**, 188 (1998).
- ⁵H. Riechert, A. Ramakrishnan, and G. Steinle, *Semicond. Sci. Technol.* **17**, 892 (2002).
- ⁶H. D. Sun, G. J. Valentine, R. Macaluso, S. Calvez, D. Burns, M. D. Dawson, T. Jouhti, and M. Pessa, *Opt. Lett.* **27**, 2124 (2002); A. H. Clark, S. Calvez, N. Laurand, R. Macaluso, H. D. Sun, M. D. Dawson, T. Jouhti, J. Kontinen, and M. Pessa, *IEEE J. Quantum Electron.* **40**, 878 (2004); J. M. Hopkins, S. A. Smith, C. W. Jeon, H. D. Sun, D. Burns, S. Calvez, M. D. Dawson, T. Jouhti, and M. Pessa, *Electron. Lett.* **40**, 30 (2004).
- ⁷M. Fisher, M. Reinhardt, and A. Forchel, *IEEE J. Sel. Top. Quantum Electron.* **7**, 149 (2001); *Electron. Lett.* **36**, 1208 (2002); D. Gollub, M. Fisher, and A. Forchel, *ibid.* **38**, 1183 (2002).
- ⁸Y. Ikenaga, T. Miyamoto, S. Makino, T. Kayeyama, M. Arai, F. Koyama, and K. Iga, *Jpn. J. Appl. Phys., Part 1* **41**, 664 (2002).
- ⁹E. Tournié, M.-A. Pinault, M. Lüigt, J.-M. Chauveau, A. Trampert, and K. H. Ploog, *Appl. Phys. Lett.* **82**, 1845 (2003).
- ¹⁰W. Zhou, K. Uesugi, and I. Suemune, *Appl. Phys. Lett.* **83**, 1992 (2003).
- ¹¹H. Y. Liu, M. Hopkinson, P. Navaretti, M. Gutierrez, J. S. Ng, and J. P. R. David, *Appl. Phys. Lett.* **83**, 4951 (2003).
- ¹²J. -Y. Duboz, J. A. Gupta, Z. R. Wasilewski, J. Ramsey, R. L. Williams, G. C. Aers, B. J. Riel, and G. I. Sproule, *Phys. Rev. B* **66**, 085313 (2002).
- ¹³J. Wu, W. Shan, W. Walukiewicz, K. M. Yu, J. W. Ager III, E. E. Haller, H. P. Xin, and C. W. Tu, *Phys. Rev. B* **64**, 085320 (2001).
- ¹⁴Z. Pan, L. H. Li, Y. W. Lin, B. Q. Sun, D. S. Jiang, and W. K. Ge, *Appl. Phys. Lett.* **78**, 2217 (2001).
- ¹⁵M. Hetterich, M. D. Dawson, A. Yu. Egorov, D. Bernklau, and H. Riechert, *Appl. Phys. Lett.* **76**, 1030 (2000).
- ¹⁶P. J. Klar, H. Gruning, W. Heimbrodt, J. Koch, W. Stolz, S. Tomic, and E. P. O'Reilly, *Solid-State Electron.* **47**, 437 (2003).
- ¹⁷H. D. Sun, M. D. Dawson, M. Othman, J. C. L. Yong, J. M. Rorison, P. Gilet, L. Grenouillet, and A. Million, *Appl. Phys. Lett.* **82**, 376 (2003); H. D. Sun, M. Hetterich, M. D. Dawson, A. Yu. Egorov, D. Bernklau, and H. Riechert, *J. Appl. Phys.* **92**, 1380 (2002).
- ¹⁸W. Shan, W. Walukiewicz, and J. W. Ager III, *Phys. Rev. Lett.* **82**, 1221 (1999).
- ¹⁹E. P. O'Reilly and A. Lindsay, *Phys. Status Solidi B* **216**, 131 (1999); A. Lindsay and E. P. O'Reilly, *Solid State Commun.* **112**, 443 (1999).
- ²⁰M. J. Joyce, M. J. Johnson, M. Gal, and B. F. Usher, *Phys. Rev. B* **38**, 10978 (1988).
- ²¹I. Vurgaftman and J. R. Meyer, *J. Appl. Phys.* **94**, 3675 (2003).
- ²²R. Asomoza, V. A. Elyukhin, and R. Pena-Sierra, *Appl. Phys. Lett.* **81**, 1785 (2002).
- ²³I. L. Krestnikov, R. Heitz, N. N. Ledentsov, A. Hoffmann, A. M. Mintairov, T. H. Kosel, J. L. Merz, I. P. Soshnikov, and V. M. Ustinov, *Appl. Phys. Lett.* **83**, 3728 (2003).
- ²⁴H. D. Sun, S. Calvez, M. D. Dawson, P. Gilet, L. Grenouillet, and A. Million (unpublished).
- ²⁵T. Kitatani, M. Kondow, and T. Tanaka, *J. Cryst. Growth* **221**, 491 (2000).
- ²⁶N. J. Y. D. Jang, D. Lee, K. H. Park, W. G. Jeong, and J. W. Jang, *Appl. Phys. Lett.* **83**, 3114 (2003).
- ²⁷L. Nasi, C. Ferrari, L. Lazzarini, and G. Clarke, *J. Appl. Phys.* **92**, 7678 (2002).
- ²⁸S. Tundo, M. Mazzer, L. Nasi, L. Lazzarini, G. Salviate, C. Rohr, P. Abbott, D. B. Bushnell, K. W. J. Barnham, G. Clarke, and R. Peng, *J. Appl. Phys.* **94**, 6341 (2003).
- ²⁹I. A. Buyanova, M. Izadifard, W. M. Chen, A. Polimeni, M. Capizzi, H. P. Xin, and C. W. Tu, *Appl. Phys. Lett.* **82**, 3662 (2003).